Electron penetration in the nucleus and its effect on the quadrupole interaction

Katrin Koch,[1,][*] Klaus Koepernik,[2] Dimitri Van Neck,[3] Helge Rosner,[1] and Stefaan Cottenier[3, 4, †]

[1]*Max Planck Institute for Chemical Physics of Solids, Nöthnitzer Str. 40,*
DE-01187 Dresden, Germany
[2]*IFW Dresden, Institute for Solid State Research, P.O. Box 270116,*
DE-01171 Dresden, Germany
[3]*Center for Molecular Modeling, Ghent University, Proeftuinstraat 86,*
BE-9000 Ghent, Belgium
[4]*Instituut voor Kern- en Stralingsfysica and INPAC,*
K.U.Leuven, Celestijnenlaan 200 D, BE-3001 Leuven, Belgium
(Dated: August 28, 2009)

A series expansion of the interaction between a nucleus and its surrounding electron distribution provides terms that are well-known in the study of hyperfine interactions: the familiar quadrupole interaction and the less familiar hexadecapole interaction. If the penetration of electrons into the nucleus is taken into account, various corrections to these multipole interactions appear. The best known one is a scalar correction related to the isotope shift and the isomer shift. This paper discusses a related tensor correction, which modifies the quadrupole interaction if electrons penetrate the nucleus: the quadrupole shift. We describe the mathematical formalism and provide first-principles calculations of the quadrupole shift for a large set of solids. Fully relativistic calculations that explicitly take a finite nucleus into account turn out to be mandatory. Our analysis shows that the quadrupole shift becomes appreciably large for heavy elements. Implications for experimental high-precision studies of quadrupole interactions and quadrupole moment ratios are discussed. A literature review of other small quadrupole-like effects is presented as well.

PACS numbers:

I. INTRODUCTION

Atomic nuclei are no mathematical point charges, but objects with a shape and a size. This affects the way in which they interact with electrons, especially when electrons penetrate the nuclear volume and render the usual 'far-field' approximation invalid. These 'near-field' effects lead to tiny corrections to all terms in the multipole expansion for the electrostatic interaction between nuclei and electrons. The correction to the monopole term corresponds to experimentally well-known phenomena: the isotope shift in atomic spectroscopy and the isomer shift in Mössbauer spectroscopy. An analogous correction to the quadrupole term – coined here the *quadrupole shift* [96] (QS) – should exist as well. The existence of such an effect has been touched upon a few times in the literature of the past decades [1, 2, 3, 4, 5, 6], but to our knowledge a systematic study is lacking. In this paper, we present a mathematical treatment of the quadrupole shift by a twofold application of first-order perturbation theory, which leads to a simple analytical expression (Secs. II-III). We point out that in order to compute numerical values for the quadrupole shift from first-principles, it is necessary to perform fully relativistic calculations that take explicitly a finite nucleus into account (Sec. IV). Density Functional Theory calculations of the quadrupole shift for a set of simple crystals show that the size of the quadrupole shift strongly grows with the mass of the isotope, an effect that turns out to have an electronic rather than a nuclear origin (Sec. V). Except for the heaviest elements (actinides), the quadrupole shift is only a minor correction to the quadrupole interaction. We discuss how it shows up in experiments, and how it could possibly be exploited to improve the accuracy of experimentally determined quadrupole moments (Sec. VI). Especially for the experimental determination of ratios between nuclear electric quadrupole moments, the accuracy that can be reached by the most precise molecular beam spectroscopy experiments is good enough to make it relevant in some cases to take quadrupole shift corrections into account. The quadrupole shift is only one of a set of small effects that can affect the regular quadrupole interaction. The (sometimes fairly old) literature on these other effects is reviewed in App. A. We suggest that for high-precision studies it is relevant to revisit these small quadrupole-like perturbations with modern computational methods.

II. FORMALISM

A. Classical interaction energy without charge-charge overlap

The *classical* electrostatic interaction energy between a positive (nuclear) charge distribution $\rho(\vec{r})$ and a potential $v(\vec{r})$ due to a surrounding (electron) charge distribution $n(\vec{r}')$ is formally given by (with ϵ_0 being the electric

---
[*]Electronic address: Katrin.Koch@cpfs.mpg.de
[†]Electronic address: Stefaan.Cottenier@ugent.be

constant)

$$E = \int \rho(\vec{r})v(\vec{r})d\vec{r} = \frac{1}{4\pi\epsilon_0} \int \int \frac{\rho(\vec{r})n(\vec{r}')}{|\vec{r} - \vec{r}'|}d\vec{r}d\vec{r}', \quad (1)$$

and can be expressed by the standard multipole expansion in spherical harmonics [7]:

$$\frac{1}{|\vec{r} - \vec{r}'|} = \sum_{l,m} \frac{4\pi}{2l + 1} \frac{r_<^l}{r_>^{l+1}}Y_{l,m}^*(\Omega)Y_{l,m}(\Omega'), \quad (2)$$

with $r_< = \min(r, r')$ and $r_> = \max(r, r')$. This leads to an infinite sum of double integrals, each with the dimen-

sion of energy:

$$E = \sum_{l=0}^{\infty} E_{2l} = E_0 + E_2 + E_4 + \dots \quad (3)$$

(Odd terms will vanish in the cases of interest here, see Sec. II B.) It is the second term E_2 that will be of interest in the present work:

$$E_2 = h\nu_Q = \frac{1}{4\pi\epsilon_0} \frac{4\pi}{5} \sum_{m=-2}^{+2} \int \int \rho(\vec{r})n(\vec{r}')\frac{r_<^2}{r_>^3}Y_{2,m}^*(\Omega)Y_{2,m}(\Omega')d\vec{r}d\vec{r}'. \quad (4)$$

The frequency ν_Q is experimentally accessible, and is called the *nuclear quadrupole coupling constant* (NQCC). Due to the varying assignment of $r_<$ and $r_>$ to 'nuclear' (r) or 'electron' (r') coordinates, quantities as E_2 are an intricate mixture of properties of both charge distributions $\rho(\vec{r})$ and $n(\vec{r})$. Only in the special case where both charge distributions do not overlap ($r_< \equiv r$ and $r_> \equiv r'$), Eq. (1) can be written in terms of properties that depend entirely on only one of the charge distributions:

$$E = \sum_{l,m} Q_{lm}^* V_{lm} , \quad (5)$$

where Q_{lm} and V_{lm} are the components of the nuclear multipole moment and electric multipole field tensors of rank l, respectively:

$$Q_{lm} = \sqrt{\frac{4\pi}{2l + 1}} \int r^l \rho(\vec{r})Y_{lm}(\Omega)d\vec{r} \quad (6)$$

$$V_{lm} = \frac{1}{4\pi\epsilon_0}\sqrt{\frac{4\pi}{2l + 1}} \int \frac{1}{r'^{l+1}}n(\vec{r}')Y_{lm}(\Omega')d\vec{r}'. \quad (7)$$

When this formalism is applied to describe nuclei and electrons, the simplification by Eq. (5) can never be made: s-electrons and relativistic $p_{\frac{1}{2}}$-electrons have a non-zero probability to appear at $r = 0$, and therefore the nuclear and electron charge distributions always overlap. Nevertheless, motivated by the very small size of the region where this overlap happens compared to the volume of the rest of the atom, one can in a first approximation neglect this concern and apply Eq. (5) to atoms, molecules and solids. This is where the concept originates of an electric-field gradient (EFG) tensor (V_{2m}) that interacts with a nuclear quadrupole moment tensor (Q_{2m}) to produce an experimentally observable interaction energy (E_2). Although E_2 itself is a well-defined

observable property, its description by a quadrupole interaction energy only

$$E_2 \approx \sum_{m=-2}^{+2} Q_{2m}^* V_{2m} \quad (8)$$

rather than by Eq. (4) is an approximation.

B. Overlap corrections

We will now derive explicit expressions for the corrections that need to be added to Eq. (8) to obtain Eq. (4) (and similarly for other values of l). Rather than using the multipole expansion in spherical harmonics from Eq. (2), we start from a Taylor expansion of the electrostatic potential $v(\vec{r}) = 1/(4\pi\epsilon_0) \int n(\vec{r}')/|\vec{r} - \vec{r}'| \ d\vec{r}'$ in the interaction energy of Eq. (1):

$$E = \int \rho(\vec{r})v(\vec{r})d\vec{r} = v(0) \int \rho(\vec{r})d\vec{r}$$
$$+ \sum_i v_i(0) \int x_i \rho(\vec{r})d\vec{r}$$
$$+ \frac{1}{2!} \sum_{i,j} v_{ij}(0) \int x_i x_j \rho(\vec{r})d\vec{r}$$
$$+ \frac{1}{3!} \sum_{i,j,k} v_{ijk}(0) \int x_i x_j x_k \rho(\vec{r})d\vec{r}$$
$$+ \frac{1}{4!} \sum_{i,j,k,l} v_{ijkl}(0) \int x_i x_j x_k x_l \rho(\vec{r})d\vec{r} + \mathcal{O}(6). \quad (9)$$

In order to recognize in this expression the multipole moments and multipole fields from Eq. (6) and Eq. (7), one

has to make substitutions like this one (the example is for the quadrupole moment):

$$\int x_i x_j \rho(\vec{r}) d\vec{r} = \frac{1}{3} \underbrace{\int (3x_i x_j - r^2 \delta_{ij}) \rho(\vec{r}) d\vec{r}}_{Q_{ij}}$$
$$+ \frac{1}{3} \int r^2 \rho(\vec{r}) d\vec{r}\, \delta_{ij}\,, \qquad (10)$$

where Q_{ij} are the components of the quadrupole tensor Q_{2m} (Eq. (6)), but now in Cartesian form. This yields for the first three even orders in Eq. (9) the following nuclear multipole moments in Cartesian form:

$$M = \int \rho(\vec{r}) v(\vec{r}) d\vec{r} = eZ \qquad (11)$$

$$Q_{ij} = \int (3x_i x_i - r^2 \delta_{ij}) \rho(\vec{r}) d\vec{r} \qquad (12)$$

$$H_{ijkl} = \int 3 \cdot 5(7x_i x_j x_k x_l$$
$$- f^H(x_i, x_j, x_k, x_l)) \rho(\vec{r}) d\vec{r} \qquad (13)$$

with $f^H(x_i, x_j, x_k, x_l) = r^2 \Big[x_i x_j \delta_{kl} + x_i x_k \delta_{jl} + x_i x_l \delta_{kj} + x_j x_k \delta_{il} + x_j x_l \delta_{ik} + x_k x_l \delta_{ij} \Big] - \frac{r^4}{5} \Big[\delta_{ij} \delta_{kl} + \delta_{ik} \delta_{jl} + \delta_{il} \delta_{jk} \Big]$. The corresponding electric multipole fields in Cartesian form are:

$$V = v(0) \qquad (14)$$

$$V_{ij} = (\partial_i \partial_j v(0) - \frac{1}{3} \Delta \delta_{ij}) \Delta v(0) \qquad (15)$$

$$V_{ijkl} = \partial_i \partial_j \partial_k \partial_l v(0) - f^V_{ijkl} \Delta v(0) \qquad (16)$$

with $f^V_{ijkl} = \Big[\partial_i \partial_j \delta_{kl} + \partial_i \partial_k \delta_{jl} + \partial_i \partial_l \delta_{kj} + \partial_j \partial_k \delta_{il} + \partial_j \partial_l \delta_{ik} + \partial_k \partial_l \delta_{ij} \Big] - \frac{\Delta}{5} \Big[\delta_{ij} \delta_{kl} + \delta_{ik} \delta_{jl} + \delta_{il} \delta_{jk} \Big]$. The expressions in Eqs. (11) to (13) and Eqs. (14) to (16) are identical to the ones in Eqs. (6) and (7), respectively. They have the same number of degrees of freedom: 1, 5 and 9 for the zeroth, second and fourth order moment/field.

After having inserted into Eq. (9) all substitutions as in Eq. (10), the interaction energy can be written as

$$E = \underbrace{M \cdot V}_{\text{MI}} + \underbrace{\frac{1}{3!}\{r^2\}\Delta v(0)}_{\text{MS}^{(1)}} + \underbrace{\frac{1}{5!}\{r^4\}\Delta^2 v(0)}_{\text{MS}^{(2)}}$$

$$+ \underbrace{\frac{1}{2!}\frac{1}{3}\sum_{ij} Q_{ij} V_{ij}}_{\text{QI}}$$

$$+ \underbrace{\frac{1}{28}\sum_{ij}\{(x_i x_j - \frac{r^2}{3}\delta_{ij})r^2\}(\partial_i \partial_j - \frac{\Delta}{3}\delta_{ij})\Delta v(0)}_{\text{QS}^{(1)}}$$

$$+ \underbrace{\frac{1}{4!}\frac{1}{105}\sum_{ijkl} H_{ijkl} V_{ijkl}}_{\text{HDI}} + \mathcal{O}(6), \qquad (17)$$

where all integrations over the nuclear charge density $\rho(\vec{r})$ are noted in short-hand by {curled brackets}. Eq. (17) contains no odd order terms (dipole, octupole,...), since nuclei have no odd order electric moments due to time reversal symmetry [3]. We see that Eq. (17) contains dot products between multipole moments and fields as in Eq. (5): the monopole (MI), quadrupole (QI), hexadecapole (HDI),... interactions. These are the only contributions in the case without charge-charge overlap. Additionally, an infinite set of even order correction terms appears now as well – due to parity, there are no odd order corrections. In Tab. I, a general naming system and a corresponding set of symbols are presented: the nth order *quasi* multipole *moment* multiplied (dot product) with the nth order *quasi* multipole *field* leads to the nth order multipole *shift*. From the general trends in this table one can infer the structure of the higher order corrections that were not explicitly derived in Eq. (17) – they are shown in the table in red.

There is a qualitative difference between the multipole fields in the first column of Tab. I and the quasi multipole fields in all other columns. The multipole fields depend on the potential $v(0)$ at the nucleus, which depends via integration on the charge distribution everywhere else in the system. Multipole fields are therefore integrated quantities, determined by the entire density. The quasi multipole fields depend on the Laplacian of the potential at the nucleus ($\Delta v(0)$), which is by the Poisson equation proportional to the electron charge density at the nucleus ($n(0)$) ($\Delta v(0) = -n(0)/\epsilon_0$). Quasi multipole fields are therefore point quantities, determined by the electron density in a single point only.

In the next section, the results of Eq. (17) and Tab. I for a system of two classical charge distributions will be translated to a quantum formulation. This will make it applicable to atoms, molecules and solids. Known experimental consequences of these overlap correction terms will be summarized in Sec. III. The core of the present work deals with the first order quadrupole shift $\text{QS}^{(1)}$, which is the first order correction to the quadrupole interaction.

C. Quantum formulation

In order to translate Eq. (17) to quantum mechanics, Hamiltonian operators corresponding to all its terms are required. The structure of Eq. (17) suggests a perturbation theory treatment, with the monopole interaction term as the unperturbed Hamiltonian, and the other terms as small perturbations. The monopole term depends via r^0 on the (small) nuclear coordinate ($r \propto 10^{-15}$ m) and via $1/r'$ on the electronic coordinate ($r' \propto 10^{-10}$ m). Among all small corrections in Tab. I, the two largest ones are the quadrupole interaction QI and the first order monopole shift $\text{MS}^{(1)}$ – both have a r^2 in their nuclear parts and a second derivative of the electrostatic potential (leading to $1/r'^3$) in their electronic

TABLE I: Systematic overview of nuclear multipole and quasi multipole moments and electric multipole and quasi multipole fields that appear in the multipole expansion of two interacting (and overlapping) classical charge distributions. The first column gives the regular multipole expansion for point nuclei: the monopole, quadrupole and hexadecapole interactions. The next columns give the quasi multipole moments/fields for every multipole interaction, denoted by a tilde: these are corrections to the multipole interactions due to electron penetration into an extended nucleus. Colored text is by generalization only, and is not systematically derived in this work. The objects in each line are spherical tensors of a given rank (rank 0 for line 1, rank 2 for line 2, rank 4 for line 3, …).

Order	Multipole moment / field	First order quasi moment / quasi field	Second order quasi moment / quasi field	…
$\mathcal{O}(0)$	MI: $M \propto r^0 Y_{00}$ $V \propto v(0)$	MS$^{(1)}$: $\tilde{M}^{(1)} \propto \{r^2 Y_{00}\}$ $\tilde{V}^{(1)} \propto \Delta v(0)$	MS$^{(2)}$: $\tilde{M}^{(2)} \propto \{r^4 Y_{00}\}$ $\tilde{V}^{(2)} \propto \Delta^2 v(0)$	…
$\mathcal{O}(2)$	QI: $Q \propto r^2 Y_{20}$ $V_{ij} \propto \partial_{ij} v(0)$	QS$^{(1)}$: $\tilde{Q}^{(1)} \propto \{r^4 Y_{20}\}$ $\tilde{V}_{ij}^{(1)} \propto \partial_{ij} \Delta v(0)$	QS$^{(2)}$: $\tilde{Q}^{(2)} \propto \{r^6 Y_{20}\}$ $\tilde{V}_{ij}^{(2)} \propto \partial_{ij} \Delta^2 v(0)$	…
$\mathcal{O}(4)$	HDI: $H \propto r^4 Y_{40}$ $V_{ijkl} \propto \partial_{ijkl} v(0)$	HDS$^{(1)}$: $\tilde{H}^{(1)} \propto \{r^6 Y_{40}\}$ $\tilde{V}_{ijkl}^{(1)} \propto \partial_{ijkl} \Delta v(0)$	HDS$^{(2)}$: $\tilde{H}^{(2)} \propto \{r^8 Y_{40}\}$ $\tilde{V}_{ijkl}^{(2)} \propto \partial_{ijkl} \Delta^2 v(0)$	…
…	…	…	…	…

parts. These two leading corrections will be taken as the small perturbation.

The Hamiltonians that correspond to the entries in Tab. I operate on the direct product space of wave functions for the nuclear and the electron subspaces. The ground state of the monopole Hamiltonian is a direct product between the nuclear ground state and the electronic ground state wave function. With $\hat{M} = eZ\hat{\mathbb{1}}$ (Eq. (11), $\hat{\mathbb{1}}$ is the identity operator on the nuclear space) and $\hat{V} = \hat{v}(0)$ (Eq. (14), $\hat{v}(0)$ is an operator on the electronic space that returns the potential at $\vec{r} = \vec{0}$ due to a given wave function Ψ), the unperturbed monopole interaction Hamiltonian is

$$\hat{\mathcal{H}}_{MI} = eZ \ \hat{\mathbb{1}} \otimes \hat{v}(0). \tag{18}$$

Evaluating this for the ground state wave function $|I \otimes \Psi_0\rangle$ of the combined nuclear+electronic system leads to ($|I\rangle$ is the ground state of the nucleus, and $|\Psi_0\rangle$ the ground state of the electron system with a point nucleus):

$$
\begin{aligned}
E_0^{pn} &= \langle \Psi_0 \otimes I | \hat{\mathcal{H}}_{MI} | I \otimes |\Psi_0\rangle \\
&= \langle I | eZ \ \hat{\mathbb{1}} | I \rangle \cdot \langle \Psi_0 | \hat{v}(0) | \Psi_0 \rangle \\
&= eZ v(0) ,
\end{aligned}
\tag{19}
$$

which is the leading term in Eqs. (5) or (17). The label pn ('point nucleus') emphasizes the difference with E_0 from

Eq. (3). The quantity $v(0)$ – the electrostatic potential at the nuclear site for a point nucleus – is accessible by first-principles codes.

The perturbing Hamiltonian is (see Tab. I for the notation):

$$\hat{\mathcal{H}}_P = \hat{\mathcal{H}}_{QI} + \hat{\mathcal{H}}_{MS^{(1)}}. \tag{20}$$

In first order perturbation theory, the energy corrections due to this perturbation are found by evaluating the perturbing Hamiltonian in the ground state of the unperturbed Hamiltonian. Assuming a non-degenerate ground state in the electron subspace, it is advantageous to write the Hamiltonians immediately in a more familiar form where the electronic matrix elements are already evaluated and are treated as known (=computable) quantities. After similar algebra as for the monopole Hamiltonian, this leads to this form for the monopole shift Hamiltonian (it contains the mean square radius $\langle r^2 \rangle$ of the nucleus and the electron density $n(0)$ at the position of the nucleus):

$$\hat{\mathcal{H}}_{MS^{(1)}} = -\frac{eZ}{6\epsilon_0} n(0) \ \langle r^2 \rangle \hat{\mathbb{1}}. \tag{21}$$

The quadrupole Hamiltonian $\hat{\mathcal{H}}_{QI}$ contains the (spectroscopic) quadrupole moment of the nucleus Q and the

quadrupole field of the electrons V_{zz} (principle component of the electric-field gradient tensor) (see e.g. Ref.[7]):

$$\hat{\mathcal{H}}_{QI} = \frac{eQV_{zz}}{4(2I-1)I\hbar^2}\left[\left(3\hat{I}_z^2 - \hat{I}^2\right) + \frac{1}{2}\eta\left(\hat{I}_+^2 + \hat{I}_-^2\right)\right]. \tag{22}$$

Diagonalizing these two Hamiltonians in the nuclear states leads to the desired energy corrections in first order perturbation. Formally:

$$\begin{aligned} E^{[1]} &= E_0^{pn} + \langle I|\hat{\mathcal{H}}_{MS^{(1)}} + \hat{\mathcal{H}}_{QI}|I\rangle \\ &= E_0^{pn} + \langle I|\hat{\mathcal{H}}_{MS^{(1)}}|I\rangle + \langle I|\hat{\mathcal{H}}_{QI}|I\rangle \end{aligned}$$

$$= E_0^{pn} + E_{MS^{(1)}}^{[1]} + E_{QI}^{[1]}. \tag{23}$$

Here, $E_{MS^{(1)}}^{[1]}$ is a correction to the monopole energy E_0^{pn} for a point nucleus due to (s- or $p_{\frac{1}{2}}$-)electron penetration into the volume of a spherical nucleus. The quadrupole interaction energy $E_{QI}^{[1]}$ is a correction due to the deviation from spherical symmetry of this nucleus.

There is a second group of entries with even much smaller corrections in Tab. I: the HDI, QS$^{(1)}$ and MS$^{(2)}$ terms all have r^4 and 4 derivatives of the electrostatic potential ($\rightarrow 1/r'^5$). The corresponding Hamiltonians are:

$$\hat{\mathcal{H}}_{HDI} = \frac{eHV_{zzzz}}{128I(I-1)(2I-1)(2I-3)\hbar^4}\cdot\left[35\hat{I}_z^4 - 30\hat{I}_z^2\hat{I}^2 + 3\hat{I}^4 + 25\hbar^2\hat{I}_z^2 - 6\hbar^2 I^2\right] \tag{24}$$

$$\hat{\mathcal{H}}_{QS^{(1)}} = -\frac{1}{14\epsilon_0}\frac{e\tilde{Q}n_{zz}}{4(2I-1)I\hbar^2}\left[\left(3\hat{I}_z^2 - \hat{I}^2\right) + \frac{1}{2}\eta_{QS}\left(\hat{I}_+^2 + \hat{I}_-^2\right)\right] \tag{25}$$

$$\hat{\mathcal{H}}_{MS^{(2)}} = -\frac{eZ}{5!\epsilon_0}\Delta n(0)\,\langle r^4\rangle\hat{\mathbb{1}}. \tag{26}$$

The (diagonal part of the) hexadecapole Hamiltonian, Eq. (24), is taken from the literature [8], the quadrupole shift Hamiltonian, Eq. (25), is derived explicitly in [9] and similar algebra as for the first order monopole shift Hamiltonian leads to the second order monopole shift Hamiltonian, Eq. (26). As they are much smaller than the QI and MS$^{(1)}$ terms, it makes little sense to add these corrections to the Hamiltonian of Eq. (20) right away. Rather one should consider a first order perturbation to the Hamiltonian of Eq. (20), which itself was already a perturbation to the monopole Hamiltonian of Eq. (18). This means: find the perturbed eigen states of Eq. (20) in first order, and evaluate the new perturbations as given by the Hamiltonians in Eqs. (24)–(26) in these eigen states. In the present work, we are interested in the first place in $\hat{\mathcal{H}}_{QS^{(1)}}$, as it has the symmetry of a quadrupole interaction: *this Hamiltonian, evaluated in the (approximate) eigenstates for a system with a finite and quadrupolarly deformed nucleus, gives an additional contribution to the regular quadrupole interaction.* It can be interpreted as the influence on the quadrupole interaction of electron penetration into the nuclear volume: the quadrupole shift. The quadrupole shift Hamiltonian of Eq. (25) expresses the influence of the finite nucleus on the multipole expansion. Evaluating this Hamiltonian for a density obtained from a first-principles calculation with a finite nucleus expresses the influence of the finite nucleus on the electronic wave functions.

There is an alternative way to express this same effect: consider the Hamiltonian of Eq. (20) up to second order perturbation. Among others, the second order energy ex-pression will contain a cross term between QI and MS$^{(1)}$, which has the same symmetry as the quadrupole interaction (this can be easily seen because the Y$_{00}$ term of the monopole shift is a scalar quantity that does not change the symmetry). Compared to the previous strategy this method has the advantage that the same Hamiltonian is kept, but the disadvantage that second order matrix elements in excited states have to be evaluated. It is technically easier to evaluate a new perturbation in the ground state of the previous perturbation. The underlying physics, however, is the same.

The second order perturbation description has been applied in 1970 by P. Pyykkö for approximate and non-relativistic calculations in a few test molecules (see also Fig. 4) [1]. The first order + first order perturbation description has been used in 2003 by Thyssen *et al.* [5] for the case of LiI, albeit in an implicit way that did not clearly showed the twofold application of first order perturbation theory. The twofold application of perturbation theory will be the method used in the present work as well, not at least because it leads to concise analytical formulas. In 2006, also Karl and Novikov derived the so-called "contact terms" of the quadrupole interaction. They used the Feynman diagram technique and evaluated the results for hyperonic atoms [10, 11]. Our derivation was made completely independent from the ones by Thyssen *et al.* and Karl and Novikov, and the observation that the final expressions agree is a strong test of mutual correctness.

D. Zooming in on E_2

The regular quadrupole interaction and first order quadrupole shift together provide our approximation to E_2:

$$E_2 = h\nu_Q \approx E_{QI} + E_{QS^{(1)}} = h\nu_{QI} + h\nu_{QS^{(1)}}. \tag{27}$$

Both terms consist each of a product between a nuclear quantity and an electron quantity. As this shows to which nuclear and/or electronic properties one gets access by measuring E_2, we discuss them now. The two relevant nuclear quantities are (see Eqs. (22) and (25)):

$$\hat{\mathcal{H}}_{QI} \rightarrow eQ = \int \rho(\vec{r})(3z^2 - r^2)d\vec{r} \propto \langle r^2 Y_{20} \rangle \tag{28}$$

$$\hat{\mathcal{H}}_{QS^{(1)}} \rightarrow e\tilde{Q} = \int \rho(\vec{r})(3z^2 - r^2)r^2 d\vec{r} \propto \langle r^4 Y_{20} \rangle. \tag{29}$$

The quasi quadrupole moment $\tilde{Q}$ has an additional r^2 in the integral compared to the quadrupole moment Q. It is therefore a quantity that bears similarity with the quadrupole moment $\langle r^2 Y_{20} \rangle$ (through the Y_{20}-dependence) as well as with the hexadecapole moment $\langle r^4 Y_{40} \rangle$ (through the r^4-dependence).

The corresponding electronic quantities are:

$$\hat{\mathcal{H}}_{QI} \rightarrow V_{zz} = \left(\partial_{zz} - \frac{\Delta}{3}\right)v(0) \tag{30}$$

$$\hat{\mathcal{H}}_{QS^{(1)}} \rightarrow n_{zz} = -\frac{1}{\epsilon_0}\left(\partial_{zz} - \frac{\Delta}{3}\right)\Delta v(0). \tag{31}$$

The integrated quantity (cf. Sec. II B) V_{zz} is the principal component of the electric-field gradient tensor. The point quantity n_{zz} is the main component of the tensor $n_{ij} = (\partial_i \partial_j - \frac{\Delta}{3}\delta_{ij})n(0)$, which has via the Laplacian two derivatives more than the main component of the EFG tensor V_{zz}. n_{zz} can be shown to be proportional to $\langle Y_{2m}/r^5 \rangle$ and therefore bears similarities with the electric quadrupole field $\langle Y_{2m}/r^3 \rangle$ as well as with the electric hexadecapole field $\langle Y_{4m}/r^5 \rangle$, cf. Eq. (7).

III. OBSERVABLE CONSEQUENCES

All entries in the (classical) Tab. I correspond to an experimentally observable correction to the total energy. The first row lists energy corrections which are a product of scalar quantities. The leading term after the monopole contribution MI (or E_0^{pn}) is the first order monopole shift $MS^{(1)}$, which experimentally manifests its presence in the well-known isomer. The second order monopole shift $MS^{(2)}$ is only very rarely taken into account. One example where it matters is the case of muonic atoms [2, 3]
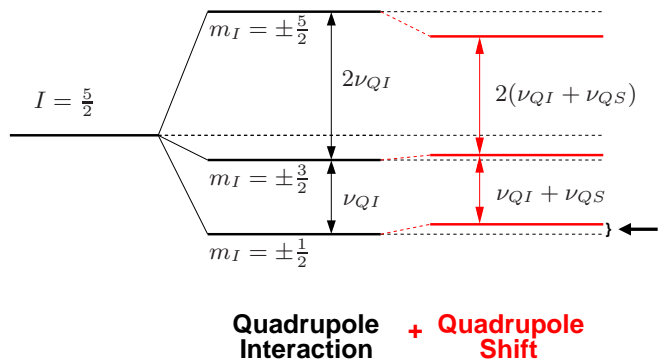

FIG. 1: Energy levels for a nuclear spin of $I = 5/2$. This picture is not on scale: the shift of the levels as indicated by the arrow is in the most favorable cases (=heavy nuclei) only 0.1 % of ν_{QI}.

(atoms where a muon rather than an electron orbits the nucleus). Because a muon is much heavier than an electron, its orbit is much smaller and the overlap with the nuclear charge distribution becomes much larger. This makes the second order monopole shift for muons much larger than it is for electrons [97].

All entries in the second row of Tab. I are dot products between spherical tensors of rank 2. The first one is the quadrupole interaction term QI, which splits according to Eq. (22) energy levels that were degenerate under the monopole term. An example for the axially symmetric case ($\eta = 0$) and nuclear spin $I = 5/2$ is given in Fig. 1. The second term in the second row is the first order quadrupole shift $QS^{(1)}$, which shifts the energy levels that were split by the quadrupole Hamiltonian, but preserves its overall symmetry (Fig. 1, example for $\eta = \eta_{QS} = 0$ [98]). The frequencies (energies) that set the scale for the quadrupole and quadrupole shift splitting are (still considering $\eta = \eta_{QS} = 0$):

$$\nu_{QI} = \frac{eQV_{zz}}{h} \tag{32}$$

$$\nu_{QS} = -\frac{e\tilde{Q}n_{zz}}{14\epsilon_0 h}. \tag{33}$$

(For the sake of lighter notation, we will use from here on ν_{QS} rather than $\nu_{QS^{(1)}}$: we will not consider second order quadrupole shifts and therefore no confusion will be possible.) The quadrupole shift does not change the overall symmetry, which in the example of Fig. 1 means that the 1:2 ratio between the two energy differences is preserved. An experiment that measures such energy differences is not able to distinguish between the contribution by ν_{QI} and the one by ν_{QS}: it measures their sum only. A discussion of the trends in the order of magnitude of the quadrupole shift will be given in Sec. V C, and several experimental and computational strategies to exploit the quadrupole shift will be suggested in Sec. VI.

Finally, the third row in Tab. I lists dot products between tensors of rank 4. The leading term here is the

hexadecapole interaction for point nuclei. This term can in principle be distinguished experimentally from a quadrupole interaction because its symmetry is different (for instance, in Fig. 1 the 1:2 ratio would be slightly violated). The HDI appears only for nuclei with $l \geq 2$, since only they have hexadecapole moments ($2I \geq l$ rule for 2^l multipole moments). Whereas the QI is well known and experimentally accessible by e.g. NMR or Molecular Beam Spectroscopy (see Sec. VI A), the situation for the HDI is different. Since it was reported in 1955 for the first time [12], it has gone through cycles of confirmatory measurements and refutations. An overview is given in Ref. [5].

IV. COMPUTATIONAL ASPECTS

A. Formulation in spherical notation

The electronic part n_{zz} of the quadrupole shift will be calculated with a first-principles code and must therefore be translated in spherical form as it is common in such codes:

$$n_{zz} = \frac{2}{\sqrt{3}} \sqrt{\frac{15}{4\pi}} \lim_{r \to 0} \frac{1}{r^2} n_{20}(r). \quad (34)$$

The spherical component of the density, $n_{20}(r)$, which enters this expression, is the radial part of the ($l=2$, $m=0$) component of expansion of the density $n(\vec{r})$ in spherical harmonics:

$$n(\vec{r}) = \sum_{lm} n_{lm}(r) Y_{lm}(\Omega). \quad (35)$$

The $l=2$ components are closely related to Cartesian second derivatives [13], which is the reason why they appear in the electric-field gradient and related quantities.

B. Computational details: the FPLO code

All calculations in this paper have been performed by the Density Functional Theory solid state code FPLO [14] (version 8.00-31), which is is a full-potential band structure scheme and based on linear combinations of overlapping non-orthogonal atom-centred orbitals. The core relaxation is properly taken into account (so called all-electron method). We used the Local Density Approximation (LDA) for the exchange-correlation functional [15]. FPLO can perform non-relativistic, scalar-relativistic as well as fully-relativistic calculations [16, 17]. In the latter, the Dirac Hamiltonian with a general potential is solved. Recently, a finite nucleus has been implemented in FPLO, which is crucial for the present work (Sec. IV C).
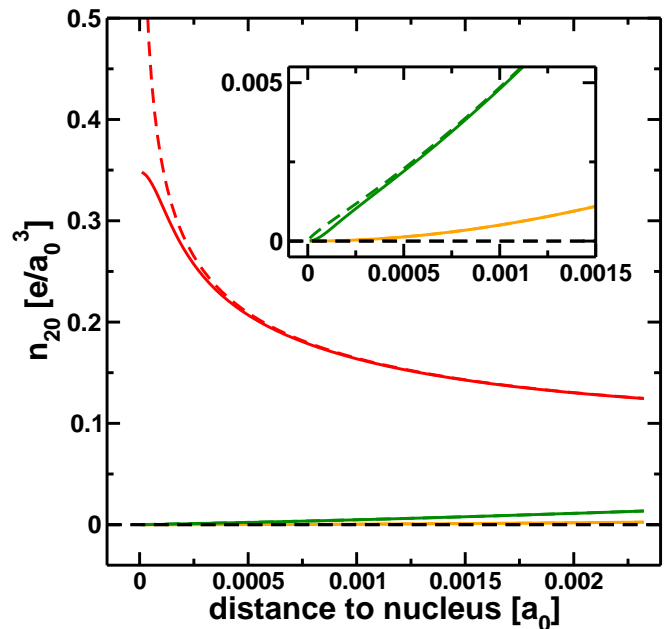

FIG. 2: The density component $n_{2m}(r)$ including inset, which zooms in the region around $r = 0$) for a point nucleus (p.n., dashed lines) and a finite nucleus (f.n., full lines) plotted in dependence of r. The different methods are indicated by different colors: non-relativistic (NREL, yellow), scalar relativistic (SREL, red) and full relativistic (FREL, green). This calculation for the hcp metal Re was done by FPLO. All quantities are given in atomic units.

C. Relativity and the role of a finite nucleus

In order to obtain n_{zz}, the limit of $n_{20}(r)/r^2$ for $r \to 0$ must be calculated, cf. Eq. (34). It matters whether this is done within a non-relativistic (NREL), a scalar-relativistic (SREL) or a fully relativistic (FREL) framework.In the NREL or FREL formulations (no matter if a point or a finite nucleus is used in the calculation) $n_{2m}(0)$ is exactly zero as it should be due to angular selection rules (Fig. 2). In the SREL approximation, the ($l=2, m$) density, created from two divergent $p_{1/2}$ functions, is to some extent wrongly non-zero at $r = 0$. This makes SREL-based methods (with or without a point nucleus) essentially useless for calculating properties that depend on $n_{20}(r \to 0)$, and we will therefore not consider SREL any further.

For a point nucleus, the ratio of $n_{20}(r)$ and r^2 converges for the limit $r \to 0$ in a NREL formulation, but not in a FREL formulation (Fig. 3). Since this ratio at $r=0$ is an observable quantity (see Eqs. (34) and (33)), the divergence for the better method (FREL vs. NREL) cannot be physical. And indeed, the divergence disappears if the approximation of a point nucleus is dropped and a finite nucleus is used in the calculation (Fig. 3). Numerical values for this ratio turn out to be much larger for FREL compared to NREL, especially for heavy elements.
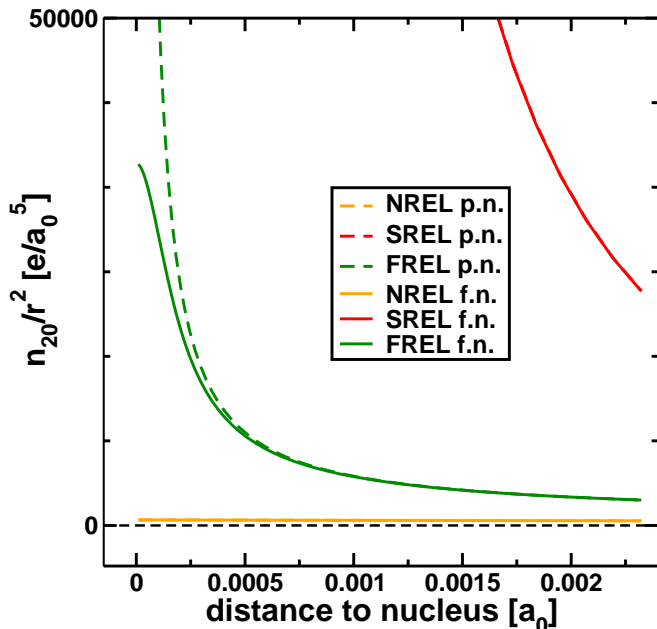
FIG. 3: The density component $n_{2m}(r)/r^2$ for a point nucleus (p.n., dashed lines) and a finite nucleus (f.n., full lines) plotted in dependence of r. The different methods are indicated by different colors: non-relativistic (NREL, yellow), scalar relativistic (SREL, red) and full relativistic (FREL, green). This calculation for the hcp metal Re was done by FPLO. All quantities are given in atomic units.

The divergence of n_{zz} in a fully relativistic point nucleus calculation might appear to be worrying at first sight. Wouldn't that mean that the quadrupole shift in Eq. (33) is infinite? The answer is: no, because the operator corresponding to n_{zz} (Eq. (31)) does not have to be evaluated in the ground state for the point nucleus (which is the case that diverges at $r = 0$), but in the ground state after having added the two perturbations of Eq. (20) that describe the effect of quadrupolarly deformed finite nucleus (where the divergence is absent). The latter ground state can be constructed from the ground and excited states of the point nucleus case, applying the common expression for the eigenfunctions in first order perturbation. This would, however, lead to rather lengthy expressions and to the inconvenience of having to use excited states. A pragmatic workaround is to use instead the ground state as calculated in a first-principles code that takes a finite nucleus into account. This is hardly an approximation, as it was exactly the purpose of the perturbations in Eq. (20) to express the presence of a finite nucleus. Therefore, we conclude that *the quadrupole shift can be obtained by evaluating the operator for n_{zz} in Eq. (31) for the ground state of the atom, molecule or solid calculated fully relativistically and with a finite nucleus taken into account.* This quadrupole shift has to be added to the contribution obtained by evaluating the operator for V_{zz} in Eq. (30) in the ground state of the point nucleus

case (and not in the ground state of the finite nucleus case, as the regular QI is really a perturbation to the point nucleus).

D.   Comparison with the PCNQM method

We have described in the previous sections a procedure to obtain the influence on the quadrupole interaction of electron penetration in a finite nucleus by two subsequent applications of first order perturbation theory combined with finite nucleus calculations (Eq. (33) and Figs. 2 and 3). An alternative to this procedure is the *point charge nuclear quadrupole moment* method (PCNQM) [18, 19, 20]: the electric-field gradient is not obtained as the expectation value of an operator, but is determined from the way how the total energy of the system changes upon inserting an artificial array of point charges around the nucleus. In this method, only total energies are required to obtain the electric-field gradient, which makes it particularly useful when the proper operator for the field gradient is not explicitly known. The latter is for instance the case as soon as a finite nucleus is used (Eq. (22) is valid for a point nucleus only), or for fully relativistic calculations at the 2-component level (a complicated and not yet performed 'picture change' transformation would be needed to find the 2-component version of the EFG operator [18].) The difference in EFGs between a 'finite nucleus + PCNQM' calculation and a point nucleus calculation (either with the regular EFG operator or with PCNQM) gives the effect of electron penetration in the nucleus. One case where this difference is explicitly calculated is for [127]I in LiI (Ref. [6] and Fig. 4). With PCNQM, the quadrupole shift can be obtained only numerically: there is no analytical expression as Eq. (33).

In passing, we note here that a method that is quite analogous to PCNQM has been recently developed for the first order monopole shift correction MS[(1)] (isotope shift, isomer shift) [21, 22] as well.

V.   NUMBERS AND TRENDS

In the present section, we will perform actual calculations with the formalism described in Secs. II and IV, and examine trends in the relevant quantities: the nuclear quasi-quadrupole moment $\tilde{Q}$, the electronic point property n_{zz}, and their product: the quadrupole shift ν_{QS}.

A.   Trends in $\tilde{Q}$

Consider a phenomenological model for a nucleus: a deformed sphere, with a radius $R(\theta)$ given by [23]:

$$R(\theta) = a\left(1 + \beta_2 Y_{20}(\theta) + \beta_4 Y_{40}(\theta) + \ldots\right), \qquad (36)$$

TABLE II: The nuclear radius a, quadrupole moment Q, deformation parameter β_2 and quasi quadrupole moment $\tilde{Q}$ of a few isotopes.

Isotope	a [fm]	Q [fm^2]	β_2	$\tilde{Q}$ [fm^4]
^{9}Be	2.84	5.3	0.22	43
^{47}Ti	4.61	30.2	0.09	644
^{111}Cd	5.95	83.0	0.07	2 934
^{138}La	6.34	45.0	0.03	1 808
^{179}Hf	6.84	379.3	0.15	17 760
^{187}Re	6.93	207.0	0.07	9 945
^{189}Os	6.95	85.6	0.03	4 138

FIG. 4: The logarithm of the ratio of ν_{QS} and ν_{QI} as a function of the mass number A. Blue diamonds: artificial crystal structures (see text and Ref. [9]), fitted by the red line (Eq. (40)). Orange triangles (down): experimental crystal structures (see Tab. III). The yellow triangle (up) [5], green square [6] and red circles [1] are values from the literature, see text. **Inset:** the same data but now as a function of Z, fit by Eq. (41). The nuclear (green) and electronic (orange) contributions of Eq. (42) are shown as well, shifted to match in the endpoint.

where a is called the monopole radius and the β_i are deformation parameters. The monopole radius depends in the first place on the atomic mass number A of the nucleus, and the main trend through a lot of experimental values can be summarized by [24][99]

$$a(A) = 1.489 \, A^{0.294} \text{ fm}. \tag{37}$$

Values for β_2 fall rarely outside the range $[-0.3, +0.3]$ (Ref. [25] in combination with Eq. (38)). As β_4 is even smaller and enters only quadratically in the expressions we will need, it can be neglected for our purposes. Keeping only the linear order for β_2, we can now express the quadrupole moment and the quasi quadrupole moment in terms of a and β_2:

$$eQ \simeq 3\sqrt{\frac{4\pi}{5}}\frac{eZ}{2\pi}\beta_2 a^2 \tag{38}$$

$$e\tilde{Q} \simeq a^2 \cdot eQ. \tag{39}$$

The term quadratic in β_2 as well as the quadratic β_4 term give corrections to Eqs. (38) and (39) at the level of a few percent only, while they make the expressions considerably more involved – see Ref. [9].

By Eqs. (38)-(39), one can get a reasonable estimate for $\tilde{Q}$ by inserting the monopole radius from Eq. (37) and the experimental quadrupole moment Q (e.g. from Ref. [25, 26, 27]). In this way, we obtain values for $\tilde{Q}$ in the order of $10^4 - 10^5$ fm^4 for heavy elements (Tab. II). The Eqs. (38)-(39) show that in order to get a large quasi quadrupole moment $\tilde{Q}$, the nucleus should be large (a is large) and strongly deformed (Q or β_2 are large). The former implies heavy elements, while the latter is most easily fulfilled for heavy elements as well.

B.   Trends in n$_{zz}$

In order to get a feeling for the order of the magnitude of the electronic parts of the $\mathcal{O}(2)$ interactions in Tab. I,
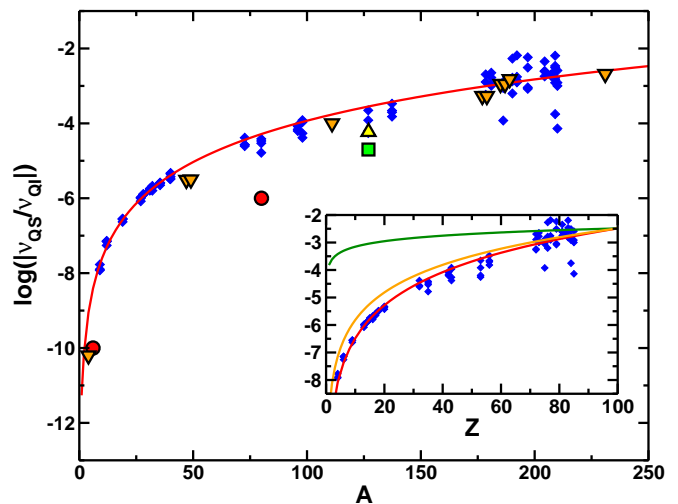
we have calculated both V_{zz} (the electronic part of the QI) and n_{zz} (the electronic part of the first order QS) for some hexagonal close-packed (hcp) metals throughout the periodic table. The results are shown in Tab. III. Both quantities increase with the mass of the element. But compared to V_{zz}, which increases over two orders of magnitude, n_{zz} is much more sensitive to the mass of the element and increases over eight orders of magnitude.

In order to verify to which extent this conclusion obtained from Tab. III is valid for other crystal structures than hcp, we investigated two series of purpose-built body-centered tetragonal (bct) crystals with different c/a ratios (0.8 and 1.2), and this for several elements throughout the periodic table. The results are reported in Ref. [9] and show the same trend as Tab. III. We conclude that the mass of the element has a larger influence on the magnitude of n_{zz} than the lattice parameters or the crystal structure.

C.   Trends in the quadrupole shift

How do the nuclear part from Sec. V A and the electronic part from Sec. V B combine to produce a quadrupole shift? The frequencies ν_{QI} (for the QI – Eq. (32)) and ν_{QS} (for the QS – Eq. (33)) for a set of hcp and bct metals are reported in Tab. III, together with their ratio $|\nu_{QS}/\nu_{QI}|$. Experimental lattice parameters were used [28, 29], and n_{zz} and V_{zz} were determined

TABLE III: For a few atoms/nuclei that experimentally condense in the hcp crystal structure (except for Pa, bct), this table lists the nuclear properties Q and $\tilde{Q}$ (determined as in Table II), the electronic properties V_{zz} and n_{zz}/ϵ_0 (calculated by FPLO, see text), the quadrupole ν_{QI} and quadrupole shift ν_{QS} frequencies they give rise to (Eqs. (32) and (33)) (mind the different MHz and kHz units), and the ratio of the latter.

Isotope	I	Q [fm^2]	$\tilde{Q}$ [fm^4]	V_{zz} [10^{21} V/m^2]	n_{zz}/ϵ_0 [10^{42} V/m^4]	ν_{QI} [MHz]	ν_{QS} [kHz]	$|\nu_{QS}/\nu_{QI}|$
^{9}Be	3/2	5	42	-0.08	$-6.07\cdot10^{-2}$	-0.1	10^{-8}	$5\cdot10^{-9}$
^{47}Ti	5/2	30	644	1.61	$3.27\cdot10^{+3}$	11.8	-0.04	$3\cdot10^{-6}$
^{49}Ti	5/2	25	539	1.61	$3.27\cdot10^{+3}$	9.6	-0.04	$3\cdot10^{-6}$
^{111}Cd	5/2	83	2 934	7.48	$2.94\cdot10^{+5}$	150.0	-14.9	$1\cdot10^{-4}$
^{177}Hf	7/2	337	15 652	7.89	$1.26\cdot10^{+6}$	642.3	-341.4	$5\cdot10^{-4}$
^{179}Hf	9/2	379	17 760	7.89	$1.26\cdot10^{+6}$	723.9	-387.4	$5\cdot10^{-4}$
^{185}Re	5/2	218	10 386	-5.51	$-1.81\cdot10^{+6}$	-290.3	324.9	$1\cdot10^{-3}$
^{187}Re	5/2	207	9 945	-5.51	$-1.81\cdot10^{+6}$	-275.6	311.1	$1\cdot10^{-3}$
^{189}Os	3/2	86	4 138	-6.65	$-2.91\cdot10^{+6}$	-137.6	208.1	$2\cdot10^{-3}$
^{231}Pa	3/2	-172	-9 357	15.14	$8.11\cdot10^{+6}$	-629.8	1309.7	$2\cdot10^{-3}$

fully relativistically with a finite nucleus for n_{zz} and a point nucleus for V_{zz} (see Sec. IV B). Q was taken from the literature [27] and $\tilde{Q}$ was determined as explained in Sec. V A. The trends of n_{zz} and $\tilde{Q}$ to be larger for heavy elements, cooperate to produce a ν_{QS} of which the relative importance with respect to ν_{QI} is rather smoothly increasing with the atomic number A.

This can be seen more clearly in Fig. 4 (blue diamonds), which summarizes results for a larger set of 28 elements in different crystal structures: hcp with c/a=1.633 and 0.8 and bct with c/a=1.2 and 0.8, always with the experimental volume per atom (details are given in Ref. [9]). These data can be fit with the simple functions

$$|\nu_{QS}| = 5.46 \cdot 10^{-12} A^{\frac{11}{3}} |\nu_{QI}|, \qquad (40)$$

$$|\nu_{QS}| = 3.26 \cdot 10^{-11} Z^4 |\nu_{QI}|, \qquad (41)$$

which are shown in Fig. 4 (red lines). The orange triangles (down) in Fig. 4 correspond to the experimental crystal structures from Tab. III – they accurately follow the same trend.

By taking the ratio of Eqs. (33) and (32) and by filling out the lowest order expressions for Q and $\tilde{Q}$ (Eq. (38)), the following simple analytic analogue for Eqs. (40) or (41) is obtained:

$$\nu_{QS} = \left(-\frac{1}{14} a^2 \frac{n_{zz}}{\epsilon_0} \frac{1}{V_{zz}}\right) \nu_{QI}. \qquad (42)$$

Since $a = 1.26 Z^{1/3}$ fm (obtained from the data of Ref. [24] plotted as a function of Z), the nuclear part a^2 scales with $Z^{2/3}$. In order to fulfill the observed Z^4 dependence in Eq. (41), the electronic part should

scale with $Z^{10/3}$: $n_{zz}/(\epsilon_0 V_{zz}) = 2.87 \cdot 10^{-10} Z^{10/3}$ fm^{-2}. These two contributions are shown as the green (nuclear) and orange (electronic) lines in the inset of Fig. 4. From this picture, it is clear that the electronic term contributes most to the increase of the quadrupole shift with A or Z. From Tab. III, we see that this is due to the strong increase of n_{zz}.

Eq. (41) provides a quick way to estimate the order of magnitude of the quadrupole shift, for any element in any crystal structure, and without the need for a finite nucleus calculation. The only quantity that is required is ν_{QI}, which can be provided by several first-principles codes. As the scatter of the data points for heavier elements shows, such an estimate can be one order of magnitude above or below the actual value. For isotopes with $A \gtrsim 175$ ($Z \gtrsim 60$), the quadrupole shift can reach 0.1-1.0% of the regular quadrupole interaction.

There are a few cases reported in the literature from which QS information can be deduced. These are shown in Fig. 4 as well. The yellow triangle (up) was calculated by J. Thyssen *et al.* with a method very similar to ours for the single case of the LiI molecule. They found the ratio $|\nu_{QS}/\nu_{QI}|$ for ^{127}I to be $5 \cdot 10^{-5}$. The green square corresponds to ^{127}I in the same LiI molecule, obtained by the PCNQM method by Van Stralen and Visscher [6]. A few estimates for the quadrupole shift obtained by second order perturbation theory were published in 1970 by P. Pyykkö [1]. Those estimates were given relative to a pseudo quadrupole interaction only (A 1 and Ref. [30]). After converting these numbers, it turns out that for the LiBr molecule the ratio of ν_{QS} and ν_{QI} is about 10^{-10} for ^{6}Li and 10^{-6} for ^{81}Br (red circles in Fig. 4). These numbers follow the same trend as the quadrupole shift in first order perturbation, but are 1-2 orders of magnitude

smaller – this might be due to the fact that these were non-relativistic calculations.

D. Other small perturbations to the quadrupole interaction

When dealing with a quadrupole-like interaction that is as small as the quadrupole shift, it becomes relevant to take into account similarly small quadrupole-like interactions and perturbations of the quadrupole interaction that have a different origin. Some of these interactions have been proposed decades ago, in an era during which it was impossible to compute accurate values for them. Given the enormous advances in the possibilities of first-principles calculations since that time, it is worthwhile to list these effects here, to discuss them shortly, to put them into a general picture and to refer to the original literature. This is done in App. A, where we will deal with second order effects of magnetic origin, the isotopologue anomaly and the influence of temperature.

VI. EXPERIMENTAL IMPLICATIONS OF THE QUADRUPOLE SHIFT

A. Accuracy of quadrupole interaction experiments and calculations

In order to see whether or not the presence of the quadrupole shift can be experimentally detected, we should assess the accuracy that can be achieved in quadrupole interaction experiments. In order to find out which kind of information can be extracted if such experiments are combined with first-principles calculations, the best achievable accuracy in such calculations will be discussed as well.

Experimental methods can be either non-radioactive ones as nuclear magnetic resonance (NMR) spectroscopy, nuclear quadrupole resonance (NQR) spectroscopy, laser spectroscopy (LS) and molecular beam spectroscopy (MBS), or radioactive ones as Mössbauer spectroscopy and perturbed angular correlation (PAC) spectroscopy. These methods can be applied to atoms and molecules (LS, MBS, NMR, NQR) or to solids (NMR, NQR, Mössbauer, PAC). A typical NQCC ν_Q is of the order of magnitude of 100 MHz. These are the lowest achievable experimental error bars on ν_Q for each method: 5 kHz for NMR or NQR on single crystals with an axially symmetric EFG [31, 32], 100 kHz for NMR or NQR on powder samples with a non-axially symmetric EFG [31, 32], 5 MHz for LS on atomic beams [33], 5-20 Hz (!) for MBS [34, 35], 500 kHz for PAC [36, 37, 38] and Mössbauer spectroscopy [39]. When compared to the the quadrupole shift values in Tab. III (typically 100 kHz for A$\gtrsim$150), it is clear that only NMR in solids and especially Molecular Beam Spectroscopy on molecules are

sensitive to the quadrupole shift – provided the isotope under consideration is sufficiently heavy.

First-principles calculations in solids are commonly done at the level of density functional theory (DFT), or with DFT as a starting point. DFT has been used with considerable success to calculate electric-field gradients in solids, see e.g. Refs. [28, 40, 41, 42, 43, 44, 45, 46, 47, 48, 49, 50, 51, 52]. As a rule of thumb, the DFT prediction is within 10% of the experimental value.

First-principles calculations for (small) molecules can resort to Hartree-Fock calculations with correlation corrections. These are computationally much more demanding, but can in principle provide an arbitrary high precision. The recent literature [53, 54, 55, 56, 57, 58] shows that correlation corrections using coupled cluster theory with single, double and (perturbatively) triple excitations (CCSD(T)), combined with sufficiently large basis sets and – where needed – with a (semi-)relativistic Hamiltonian, provides highly accurate EFGs for small molecules. It has been claimed [59] that in this way an absolute accuracy with 4 significant digits can be reached. This is considerably better than the accuracy which DFT can provide for the EFG in solids. For molecules that are too demanding for a CCSD(T) treatment, DFT with the recently proposed CAMB3LYP* functional can be an alternative [60]. DFT for EFGs in small molecules can be very unreliable [60].

At non-zero temperatures, vibrational states will be populated in solids and molecules, and in molecules rotational states as well. This will influence the electric-field gradient. In solid state calculations, this has so far only rarely been taken into account [61]. In molecules, the effect of temperature is routinely taken into account in calculations [56, 62] as well as in the analysis of experiments [63, 64, 65]. This allows an even more detailed comparison between experiment and theory for molecules.

B. Determination of Q and $\tilde{Q}$: method

With the experimental accuracies listed in the previous section, it is clear that experimental nuclear quadrupole coupling constants ν_Q for NMR on single crystals and for molecular beam spectroscopy on molecules are affected by the quadrupole shift. This means that the experimentally determined value for ν_Q would have a different value (outside the error bar) if the quadrupole shift could be "switched off". It does not mean, however, that by such an experiment the quadrupole shift itself can be determined: the QS manifests itself as an addition to the regular quadrupole interaction, and is indistinguishable from it (Eqs. (32) and (33)):

$$\nu_Q \approx \nu_{QI} + \nu_{QS} = Q\frac{eV_{zz}}{h} - \tilde{Q}\frac{en_{zz}}{14\epsilon_0 h}. \quad (43)$$

The second term of this equation is even in the most favorable cases 2-3 orders of magnitude smaller than the

first term (Fig. 4). If ν_Q is measured, if V_{zz} is calculated from first-principles and if ν_{QS} is neglected, then the quadrupole moment Q can be determined from Eq. (43). This has become the preferred procedure to determine nuclear quadrupole moments (e.g. [27, 27, 43, 60, 66, 67, 68, 69]).

If V_{zz} could be calculated with an arbitrary high precision, the precision of the resulting Q is limited by neglecting ν_{QS}. One could choose not to neglect ν_{QS}, and apply Eq. (43) to at least two ν_Q measurements in order to determine simultaneously a more precise value of Q and $\tilde{Q}$ (or Q and a^2). This would be meaningful only in cases where the absolute deviations on the computed V_{zz} and n_{zz} values are small enough to make the uncertainty in ν_{QI} smaller than the value of ν_{QS}. The only hope to realize this is in the case of sufficiently heavy elements, for which, however, it might not yet be feasible to achieve the requested computational accuracy.

C. Quadrupole moment ratios: the quadrupole anomaly

When it is not possible to know experimentally the value of a quadrupole moment with sufficient accuracy, the next best thing to know are ratios of quadrupole moments for two different isotopes, or for two different isomeric states of the same isotope. As soon as a later experiment succeeds to determine one of the quadrupole moments in the ratio, the other one is known as well.

The ratio Q_1/Q_2 of two quadrupole moments is commonly measured as the ratio $\nu_{Q,1}/\nu_{Q,2}$ of two nuclear quadrupole coupling constants. Indeed, in the absence of a quadrupole shift, both ratios are identical if the two isotopes or isomers are in the same environment and therefore experience the same V_{zz} (Eq. (43)). The presence of the quadrupole shift, however, spoils the equality of both ratios. It is straightforward to show that the ratio of quadrupole coupling constants is equal to

$$\frac{\nu_{Q,1}}{\nu_{Q,2}} = \frac{Q_1}{Q_2}\left(1+\delta\right)$$
$$\text{with} \quad \delta = \frac{n_{zz}}{14\epsilon_0 V_{zz}}\left(a_2^2 - a_1^2\right) + O\left(a_i^4\right). \quad (44)$$

This formulation is strongly reminiscent to the Bohr-Weisskopf effect [70] for magnetic hyperfine interactions, where the ratio between two *magnetic* hyperfine interaction frequencies for two isotopes/isomers at identical sites is given by

$$\frac{\nu_1}{\nu_2} = \frac{\mu_1}{\mu_2}\left(1+\Delta\right). \quad (45)$$

Here μ_1 and μ_2 are the nuclear magnetic moments of the two isotopes/isomers, and Δ is the *hyperfine anomaly*. The ratio μ_1/μ_2 can be determined from hyperfine experiments on the two free isotopes/isomers in a known externally applied magnetic field. Comparison with
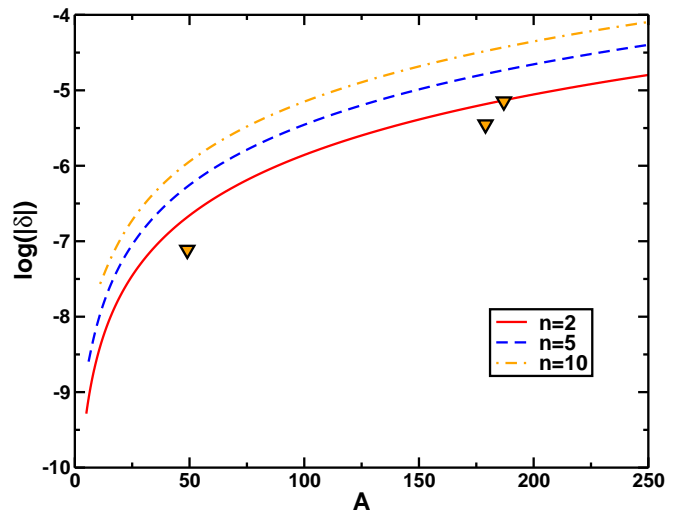

FIG. 5: The logarithm of the quadrupole anomaly δ as a function of the mass number A, as given by Eq. (46). The value of n indicates the mass number difference between the heaviest (A) and lightest ($A-n$) isotope. The curves for $n=2$ (full red line), $n=5$ (blue dashed line) and $n=10$ (yellow dot-dashed line) are shown. For ^{47}Ti, ^{179}Hf and ^{187}Re (all $n=2$) $\log|\delta|$ can be calculated explicitly from Tab. III (orange triangles).

the ratio as determined from experiments with the isotopes/isomers incorporated in solids or molecules provides the value for Δ, which can be as large as 2 % for heavy elements like ^{185,187}Re [71]. Δ is nonzero because electrons that penetrate the nucleus do not interact with a point nucleus magnetic moment but with the spatial distribution of the magnetic moment over the nuclear volume. This slightly affects the effective hyperfine field. Therefore, the hyperfine anomaly is sensitive to the details of nuclear structure, and can be used to test theoretical nuclear models.

In the same way the δ from Eq. (44) – which can be called in analogy the *quadrupole anomaly* – probes details of the nuclear charge distribution by electrons that penetrate into the nuclear volume. From Eq. (44), it can be seen that δ is sensitive to the electronic quantities, n_{zz} and V_{zz}, and the *difference* between the squared monopole radii of the two isotopes/isomers that are involved.

In order to find a general trend and order of magnitude estimate for δ, we combine the analytical function of Eq. (42) with the fitted function of Eq. (40) and the square of Eq. (37) to obtain a numerical approximation for the electronic part $n_{zz}/(14\epsilon_0 V_{zz})$ in Eq. (44). By inserting this and the square of Eq. (37) for two different isotopes in the definition of δ, the following dependence of $|\delta|$ on the isotope mass number emerges:

$$|\delta(A)| = 5.46 \cdot 10^{-12} A^{3.079}\left(A^{0.588} - (A-n)^{0.588}\right). \quad (46)$$

TABLE IV: Ratios of experimental quadrupole coupling constants for two different isotopes in two different diatomic molecules, collected from the literature. Only cases where the error bar on this ratio has been determined directly from the fit to the experimental data are reported (this error bar can be slightly different from what one would obtain using the error bars on the individual frequencies, see the discussion in Ref. [35]). The experimental value of the EFG (in $10^{21}\,\mathrm{V/m^2}$) and the estimated value of δ (Eq. (46)) are given as well.

Molecules	Isotopes	ν_{na}/ν_{ma}	V_{zz}^{exp}	$|\delta|$	Ref.
$^6\mathrm{Li}^{19}\mathrm{F}$, $^7\mathrm{Li}^{19}\mathrm{F}$	$^6\mathrm{Li}/^7\mathrm{Li}$	0.020161 ± 0.000013	-0.44	$5.9 \cdot 10^{-10}$	[72]
$^6\mathrm{Li}^{127}\mathrm{I}$, $^7\mathrm{Li}^{127}\mathrm{I}$	$^6\mathrm{Li}/^7\mathrm{Li}$	0.02028 ± 0.00014	-0.18		[63]
$^{41}\mathrm{K}^{19}\mathrm{F}$, $^{39}\mathrm{K}^{19}\mathrm{F}$	$^{41}\mathrm{K}/^{39}\mathrm{K}$	1.217699 ± 0.000055	-5.6	$1.3 \cdot 10^{-7}$	[73]
$^{41}\mathrm{K}^{127}\mathrm{I}$, $^{39}\mathrm{K}^{127}\mathrm{I}$	$^{41}\mathrm{K}/^{39}\mathrm{K}$	1.2174935 ± 0.0000099	-3.0		[74]
$^{87}\mathrm{Rb}^{19}\mathrm{F}$, $^{85}\mathrm{Rb}^{19}\mathrm{F}$	$^{87}\mathrm{Rb}/^{85}\mathrm{Rb}$	0.4838301 ± 0.0000018	-10.7	$9.6 \cdot 10^{-7}$	[35]
$^{87}\mathrm{Rb}^{35}\mathrm{Cl}$, $^{85}\mathrm{Rb}^{35}\mathrm{Cl}$	$^{87}\mathrm{Rb}/^{85}\mathrm{Rb}$	0.483837 ± 0.000022	-8.2		[75]

This expression estimates the order of magnitude of δ for two isotopes with mass numbers A and $A-n$. Curves for $\log|\delta(A)|$ for $n = 2$, 5 and 10 are shown in Fig. 5. We observe that the quadrupole anomaly strongly increases with A (or Z), due to the increase of n_{zz}. Mass number differences of 10 yield a value for δ that is an order of magnitude larger than mass number differences of 2. For the 3 elements in Tab. III for which information for 2 isotopes is provided, Eq. (46) can be compared by values obtained by filling out the quantities of Tab. III directly into Eq. (44). The values are shown by the orange triangles in Fig. 5 and correspond to the red fit ($n = 2$). This comparison shows that Eq. (46) is within one order of magnitude indeed a good estimate for δ. The experimentally achievable accuracy of quadrupole moment ratios is of the order of 10^{-6} (see Tab. IV). This means that for many isotopes the presence of δ affects the experimental values.

Unfortunately, whereas in Bohr-Weisskopf experiments the unperturbed ratio μ_1/μ_2 can be determined from experiments on free nuclei in an externally applied magnetic field, this is not possible for quadrupole interaction measurements: electric-field gradients that can be generated by man-made devices are too small to allow meaningful quadrupole interaction measurements [76]. Therefore, a slightly different method has to be used. One could perform 4 quadrupole interaction experiments on two isotopes ('m' and 'n') of the same element, each of them being part of two different molecules ('A' and 'B'). For instance, ^mX in ^mXA and ^mXB molecules, and ^nX in ^nXA and ^nXB molecules. This yields four experimental frequencies ν_m^A, ν_n^A, ν_m^B and ν_n^B. By applying Eq. (44) twice, it can be seen that the NQCC ratios are not necessarily identical to each other for the two different molecules, with the difference being determined by n_{zz}/V_{zz}:

$$\frac{\nu_m^A}{\nu_n^A} = \frac{Q_m}{Q_n}\left(1 + \frac{n_{zz}^A}{14\epsilon_0 V_{zz}^A}\left(a_n^2 - a_m^2\right)\right) \qquad (47)$$

$$\frac{\nu_m^B}{\nu_n^B} = \frac{Q_m}{Q_n}\left(1 + \frac{n_{zz}^B}{14\epsilon_0 V_{zz}^B}\left(a_n^2 - a_m^2\right)\right). \qquad (48)$$

As long as the quadrupole shift ($\propto n_{zz}$) does not play a significant role, the two experimental frequency ratios at the left-hand side are within their error bars identical to each other. If, however, the quadrupole shift would be large enough, these two experimental frequency ratios would differ from each other. *This is a completely experimental procedure to detect the presence of the quadrupole shift effect.* Tab. IV lists a collection of experimental NQCC-ratios in diatomic molecules determined for three such sets of 4 experiments, which gives an impression of the experimental accuracy that can be achieved. The estimated order of magnitude for $|\delta|$ (Eq. (46)) is given too. For none of these cases, δ is expected to be large enough to affect the experimental ratios. Tab. IV combined with Fig. 5 suggests that if the best experimental accuracies of 10^{-6} can be achieved for isotopes with A$\geq$150, then the influence of δ could be observed. The heavier the element and the larger the size-differences between the two isotopes, the more likely large δ-values are. Interestingly enough, the quadrupole coupling constant ratios for the two K isotopes in the KF and KI molecules differ from each other in the 4th digit, and this difference is an order of magnitude larger than the experimental error bars. Given the estimate for δ, the quadrupole shift is expected to give an effect in the 7th digit at best. It is therefore unlikely that this set of K-experiments represents an experimental observation of the quadrupole shift (it could be due to one of the other effects discussed in App. A, or due to an experimental problem). Nevertheless, it would be interesting to perform similar experiments with the same accuracy for heavier elements, where δ is expected to be larger.

One step further is to solve the system of the two equations (47) and (48) for the unknown quantities Q_m/Q_n

and $\left(a_n^2 - a_m^2\right)$:

$$\frac{Q_m}{Q_n} = \frac{\frac{\nu_{mb}}{\nu_{nb}}\frac{n_{zz}^a}{14\epsilon_0 V_{zz}^a} - \frac{\nu_{ma}}{\nu_{na}}\frac{n_{zz}^b}{14\epsilon_0 V_{zz}^b}}{\frac{n_{zz}^a}{14\epsilon_0 V_{zz}^a} - \frac{n_{zz}^b}{14\epsilon_0 V_{zz}^b}} \tag{49}$$

$$a_n^2 - a_m^2 = \frac{\frac{\nu_{ma}}{\nu_{na}} - \frac{\nu_{mb}}{\nu_{nb}}}{\frac{\nu_{mb}}{\nu_{nb}}\frac{n_{zz}^a}{14\epsilon_0 V_{zz}^a} - \frac{\nu_{ma}}{\nu_{na}}\frac{n_{zz}^b}{14\epsilon_0 V_{zz}^b}}. \tag{50}$$

All quantities at the right-hand side of these equations can either be measured or calculated, such that the quantities at the left-hand side are effectively determined by a combination of experiment and theory. Clearly, this is a game with very small numbers. The difference between the two frequency ratios in the numerator of Eq. (50) is of the same order of magnitude as the δ in Eq. (44): 10^{-5} for heavy elements. The same considerations as in Sec. VI B apply here: an extreme accuracy in experiments as well as in calculations is needed in order to get to a reliable conclusion. Furthermore, the procedure as described here can be disturbed by the presence of a few other small quadrupole-like effects that are discussed in Sec. V D and App. A.

VII. CONCLUSIONS AND OUTLOOK

In this work, we described how electron penetration in the nuclear volume leads to the *quadrupole shift*: a small perturbation of the regular quadrupole interaction, which depends on the second derivative of the electron charge density at the nucleus (n_{zz}), as well as on the size and shape of the nucleus ($\tilde{Q}$). An explicit expression for the quadrupole shift that can be implemented in a band structure code was derived, and DFT calculations were performed for a set of crystalline materials. It was shown that meaningful numerical values for the quadrupole shift can be obtained only for fully relativistic calculations that take a finite nucleus into account. Therefore, the quadrupole shift is one of the few cases where the commonly used scalar-relativistic approximation is definitely insufficient.

The quadrupole shift is a small effect. Its order of magnitude appears to be related in the first place to the atomic number A of the element under consideration, and to a lesser extent to the crystal structure (Fig. 4). This is predominantly due to the way how n_{zz} depends on Z. The quadrupole shift is orders of magnitude smaller than the regular quadrupole interaction for most elements, but can reach 1% to perhaps 10% near the actinide region.

We have pointed out how the quadrupole shift can play a role in a more accurate determination of quadrupole moments and quadrupole moment ratios. The comparison of two accurately measured quadrupole coupling constant ratios provides a purely experimental way to observe the presence of the quadrupole shift. For suitable cases, the required experimental accuracy can be reached by e.g. molecular beam spectroscopy. With fur-ther advances in the absolute accuracy of *ab initio* calculations for n_{zz} and V_{zz}, awareness of the existence of the quadrupole shift will help to extract more precise nuclear information from quadrupole coupling experiments.

Suggestions for further work are at the conceptual, computational as well as on the experimental level. Conceptual: it remains to be understood which features of the electron density are responsible for the observed Z-dependence of n_{zz} and for the dependence of n_{zz} for a given element on the crystal structure. Understanding those mechanisms would help to single out situations where the quadrupole shift is maximized. Computational: in the present work, only DFT calculations for solids were performed, whereas the most accurate experiments are available for molecules. DFT for molecules is not likely to provide very accurate results, but quantum chemical calculations can do much better in this respect. It would be interesting to examine for instance the value of the quadrupole shift for heavy elements in a set of molecules. Experimental: sets of 4 quadrupole coupling experiments as in Tab. IV, done for heavy elements and with high accuracy, provide a way to observe the presence of the quadrupole shift experimentally. It would be most efficient to make first a computational study, to identify among those molecules that are experimentally most easily accessible the ones where a large quadrupole shift is most likely.

APPENDIX A: OTHER SMALL PERTURBATIONS TO THE QUADRUPOLE INTERACTION

As announced in Sec. V D, this appendix discusses several other small quadrupole-like effects that might be of similar magnitude of the quadrupole shift.

1. Second order effects of magnetic origin

Van Vleck, Rabi, Foley and Ramsey [77, 78, 79] discussed half a century ago a *pseudo quadrupole interaction* in molecules that has a magnetic origin. This has been later elaborated upon by P. Pyykkö, especially for the case of metals [30, 80]. Mathematically, this pseudo quadrupole interaction arises in the same way as the quadrupole shift when the latter is derived by second order perturbation theory (see the end of Sec. II C). The small perturbing Hamiltonians are now the ones that give rise to the magnetic hyperfine field: the nuclear spin/electron orbit Hamiltonian ($\hat{\mathcal{H}}_1$), the nuclear spin/electron spin dipole-dipole Hamiltonian ($\hat{\mathcal{H}}_2$) and the Fermi contact Hamiltonian ($\hat{\mathcal{H}}_3$). In second order perturbation, the square of $\hat{\mathcal{H}}_1$, the square of $\hat{\mathcal{H}}_2$ and the cross-term of $\hat{\mathcal{H}}_2$ and $\hat{\mathcal{H}}_3$ contain an $\hat{I}_z^2$ operator that gives rise to a quadrupole-like interaction (compare to Eq. (22), provided axial symmetry ($\eta = 0$) is present). Such a term is included even in first order in $\hat{\mathcal{H}}_1$. These pseudo quadrupole interactions were shown to be at the level of 10^{-4}-10^{-6} of the regular quadrupole interaction in molecules [30, 78, 79], and reach in favorable cases up to 1% in metals [30]. The values in molecules are therefore of the same order of magnitude as the quadrupole shift (Fig. 4 and Tab. III).

Strictly spoken, these quadrupole-like contributions have a different status than the quadrupole shift in Sec. II. The quadrupole shift Hamiltonian (Eq. (25)) has exactly the same structure as the quadrupole interaction Hamiltonian (Eq. (22)), and they are therefore completely indistinguishable from each other. The quadrupole-like interactions discussed in the present section have in the first place a $\hat{I}_z^2$ dependence which splits the nuclear levels in a quadrupole-like manner as long as the environment has axial symmetry ($\eta = 0$). The important case of linear molecules has this symmetry. In less symmetrical environments, one could in principle distinguish between these quadrupole-like interactions and the quadrupole shift. As this symmetry breaking is itself a small effect, however, such considerations are not expected to be of much practical value.

For completeness, we mention two other sources of quadrupole-like interactions, which are believed [80] to be even smaller than the previously described ones: the influence of an external magnetic field [81, 82] and nuclear polarization [83].

2. The isotopologue anomaly

Through high-precision molecular beam experiments, Cederberg *et al.* have drawn attention to the fact that the quadrupole interaction at nucleus B in an AB diatomic molecule slightly depends on which isotope is taken for element A. For the isotopologues[100] $^7\text{Li}^{127}\text{I}$ and $^6\text{Li}^{127}\text{I}$, this *isotopologue anomaly* is 0.007% of the regular quadrupole interaction at ^{127}I (an absolute shift of 14 kHz) [63]. For $^{41}\text{K}^{127}\text{I}$ and $^{39}\text{K}^{127}\text{I}$, the relative effect at ^{127}I was 10 times smaller (0.0007%, absolute shift of 0.6 kHz) [74], while for $^{39}\text{K}^{81}\text{Br}$ and $^{39}\text{K}^{79}\text{Br}$ there was no effect found at all on ^{39}K [74]. The origin of the isotopologue anomaly is not understood [63, 74], but from the literature review we present in Tab. V, a correlation between the relative value of the isotopologue anomaly and the relative mass number change for the A-isotope is clearly present. The 50% relative mass change between hydrogen and deuterium results in an isotopologue anomaly of 0.2-1.0%. It tends to be lower for the 33% mass change between deuterium and tritium (0.1-0.6%), although the error bars prevent unambiguous conclusions. Much smaller but definitely non-zero frequency differences are observed for LiI and KI as well (0.007% and 0.001%). Tab. V suggests that these isotopologue anomalies tend to become undetectably small for relative mass number changes below 5%.

The isotopologue anomalies as presented in Tab. V were obtained as the difference between (ν=0, J=0)-terms in the vibrational/rotational expansion of the quadrupole coupling (see e.g. Eq. (19) in Ref. [34]). This lowest order term is not exactly equal to the static quadrupole coupling constant at the equilibrium internuclear separation, due to the presence of an additional constant (the αB^2 term in Eq. (18) of Ref. [34]) which is mass-dependent and therefore isotope-dependent. This αB^2 term could therefore be an obvious candidate to explain the observed frequency difference. However, Cederberg *et al.* have shown for CsF that αB^2 is negligible [90], because it is an order of magnitude smaller than the (ν=2, J=0)-term, which itself is experimentally known to be small. We verified that the same argument holds true for LiI ($\Delta m_{rel} = 14\%$) [34] and HI ($\Delta m_{rel} = 50\%$) [85, 91]. Therefore, it is safe to conclude that the larger as well as the smaller frequency differences in Tab. V are not significantly influenced by the αB^2 term and represent a real difference between two static quadrupole coupling constants, a difference of which the origin remains to be understood.

Isotopologue anomalies in the kHz region can be of the same order of magnitude as the quadrupole shift ν_{QS}. Their existence puts further limitations on the numerical information that can be extracted from a comparison of experimental quadrupole coupling constants and first-principles calculations. Indeed, the *first-principles* values for V_{zz} and n_{zz} that appear for instance in Eqs. (49) and (50) can only be calculated for specified *elements* in the molecule, not for the *isotopes*. On the other hand,

molecule A	molecule B	$\nu_{Q,A}$ (MHz)	$\nu_{Q,B}$ (MHz)	$\Delta\nu$ (kHz)	$\Delta\nu_{rel}$ (%)	Δm_{rel} (%)	Ref.
^{1}H^{81}**Br**	^{2}H^{81}**Br**	447.9(14)	443.363(105)	4537(1500)*	1.023%	50.0%	[84]
^{1}H^{79}**Br**	^{2}H^{79}**Br**	535.4(14)	530.648(74)	4752(1500)*	0.896%	50.0%	[84]
^{1}H^{37}**Cl**	^{2}H^{37}**Cl**	-53.436(95)	-53.037(113)	-399(200)*	0.752%	50.0%	[84]
^{1}H^{35}**Cl**	^{2}H^{35}**Cl**	-67.800(95)	-67.417(98)	-383(200)*	0.568%	50.0%	[84]
^{1}H^{127}**I**	^{2}H^{127}**I**	-1828.059(51)	-1823.226(54)	-4833(100)*	0.265%	50.0%	[85, 86]
^{2}H^{35}**Cl**	^{3}H^{35}**Cl**	-67.417(98)	-67.0(6)	-417(700)	0.622%	33.3%	[84]
^{2}H^{79}**Br**	^{3}H^{79}**Br**	530.648(74)	530(2)	648(2100)	0.122%	33.3%	[84]
^{2}H^{81}**Br**	^{3}H^{81}**Br**	443.363(105)	443(2)	363(2100)	0.082%	33.3%	[84]
^{2}H^{37}**Cl**	^{3}H^{37}**Cl**	-53.037(113)	-53.0(6)	-37(700)	0.070%	33.3%	[84]
^{6}Li^{127}**I**	^{7}Li^{127}**I**	-194.33834(20)	194.35241(20)	14.07(40)*	0.007%	14.3%	[63]
^{35}Cl^{45}**Sc**	^{37}Cl^{45}**Sc**	68.2067(29)	68.2062(29)	0.5(6.0)	0.000%	5.4%	[87]
^{39}K^{127}**I**	^{41}K^{127}**I**	-85.471138(7)	-85.471721(12)	0.583(20)*	0.001%	4.8%	[74]
^{63}CuOC-^{127}**I**	^{65}KOC-^{127}**I**	-593.465(9)	-593.485(10)	20(20)	0.003%	3.1%	[88]
^{79}Br^{39}**K**	^{81}Br^{39}**K**	-5.032957(9)	-5.032957(9)	0.000(20)	0.000%	2.5%	[74]
^{79}Br^{45}**Sc**	^{81}Br^{45}**Sc**	65.2558(32)	65.2597(38)	-3.9(7.0)	0.000%	2.5%	[89]

TABLE V: The isotopologue anomaly for a set of diatomic molecules. First two columns: the molecules with their isotopes – the isotope for which the NQCC is measured is put in bold. Second two columns: the NQCC in MHz. $\Delta\nu$: the difference between the preceding two columns (kHz) – cases where the error bar allows to conclude the difference is not zero, are labeled by a "*". $\Delta\nu_{rel}$: relative frequency difference (%). Δm_{rel}: relative change in atomic mass number for the neighboring isotope (%).

the purely experimental determination of the presence of a quadrupole shift by 4 NQCC measurements as in Eqs. (47) and (48) is not disturbed by the isotopologue anomaly, as long as one makes sure that the isotopes for A and B in the $^{(m,n)}$XA and $^{(m,n)}$XB molecules remain identical in all 4 cases.

3. Temperature and vibrations

The entire discussion so far implicitly assumed static molecules or crystals (0 K and no zero point vibrations). At non-zero temperatures, vibrational states will be populated, and in molecules rotational states as well. These will influence the electric-field gradient and therefore the quadrupole interaction. The effect is in the range of 1-10%, and should therefore certainly be taken into account in high-precision studies. In molecules, this effect can be described with high accuracy using a Schlier-Dunham treatment [34, 63, 64, 65], and quadrupole coupling experiments are routinely analyzed according to this formalism [34, 63, 85, 87, 89, 91]. Similar studies in solids are rare – see e.g. Ref. [61] for hcp-Cd, where a contribution of 1.6% due to zero-point vibrations was found.

[1] P. Pyykkö. *Chem. Phys. Lett.*, 6:479, 1970.
[2] R. M. Steffen. *Hyperfine Int.*, 9:39–52, 1981.
[3] R. M. Steffen. *Hyperfine Int*, 24-26:223–250, 1985.
[4] I. M. Band, M. A. Listengarten, and M. B. Trzhaskovskaya. *Izvestiya Akademii Nauk SSSR, Seriya Fizicheskaya*, 49:2202, 1985.
[5] J. Thyssen, P. Schwerdtfeger, M. Bender, W. Nazarewicz, and P. B. Semmes. *Phys. Rev. A*, 63(2):022505, Jan 2001.
[6] J. N. P. Van Stralen and L. Visscher. *Mol. Phys.*, 101:2115, 2003.
[7] A. Abragam. *The Principles of Nuclear Magnetism*. Oxford Univ. Pr., 1996.
[8] M.-Y. Liao and G. S. Harbison. *J. Chem. Phys.*, 100(3):1895, 1994.

[9] K. Koch. *Electron density in intermetallic compounds: chemical bonding, magnetism and the Electric Field Gradient*. PhD thesis, TU Dresden, 2009.
[10] G. Karl and V. A. Novikov. *Phys. Rev. C*, 74:024001, 2006.
[11] G. Karl and V. A. Novikov. *Phys. Rev. C*, 77:039901(E), 2008.
[12] T.-C. Wang. *Phys. Rev.*, 99(2):566–577, Jul 1955.
[13] K. Koch, R. Kuzian, K. Koepernik, I. V. Kondakova, and H. Rosner. *to be submitted to Phys. Rev. B*, 2009.
[14] K. Koepernik and H. Eschrig. *Phys. Rev. B*, 59(3):1743–1757, Jan 1999.
[15] J. P. Perdew and Y. Wang. *Phys. Rev. B*, 45:13244, 1992.
[16] K. Koepernik, H. Eschrig, I. Opahle, U. Nitzsche,

I. Chaplygin, and M. Richter. *psi-k-newsletter*, 2002.

[17] I. Opahle H. Eschrig, M. Richter. *Relativistic Electronic Structure Theory*, volume 13, chapter Relativistic Electronic Structure Theory, pages 723–776. Elsevier, 2004.

[18] M. Pernpointer, M. Seth, and P. Schwerdtfeger. *J. Chem. Phys.*, 108:6722, 1998.

[19] V. Kellö and A. J. Sadlej. *Int. J. Quant. Chem.*, 68:159, 1998.

[20] V. Kellö and A. J. Sadlej. *J. Chem. Phys.*, 112:522, 2000.

[21] M. Filatov. *J. Chem. Phys.*, 127(8):084101, 2007.

[22] R. Kurian and M. Filatov. *J. Chem. Theo. Comput.*, 4:278, 2008.

[23] P. Ring and P. Schuck. *The Nuclear Many Body Problem.* Springer-Verlag, New York, 1980.

[24] I Agneli. *Atomic Data and Nuclear Data Tables*, 87:185, 2004.

[25] N. J. Stone. *Atomic Data and Nuclear Data Tables*, 90:75, 2005.

[26] Robin K. Harris and Edwin D. Becker. *J. of Magn. Reson.*, 156:323, 2002.

[27] Pekka Pyykkö. *Molecular Physics*, 106(16-18):1965–1974, 2008.

[28] M. Ogura and H. Akai. *J. Phys.: Condens. Matter*, 17(37):5741–5755, 2005.

[29] W. H. Zachariasen. *Acta Crystallographica*, 12:698, 1959.

[30] P. Pyykkö and J. Linderberg. *Chem. Phys. Lett.*, 5:34, 1970.

[31] H. Chihara and N. Nakamura. *Nuclear Quadrupole Resonance Spectroscopy Data*, volume III/20a-c, III/31a-b, III/39 of *Landolt-Börnstein*. Springer-Verlag, 1988,1993,1997.

[32] K. J. D. MacKenzie and M. E. Smith. *Multinuclear solid-state NMR of inorganic materials.* Elsevier, 2002.

[33] Günay Başar, Gönül Başar, and Sophie Kröger. *Optics Communications*, 282:562, 2009.

[34] J. Cederberg, D. Olson, A. Nelson, D. Laine, P. Zimmer, M. Welge, M. Feig, T. Höft, and N. London. *J. Chem. Phys.*, 110:2431, 1999.

[35] J. Cederberg, E. Frodermann, H. Tollerud, K. Huber, M. Bongard, J. Randolph, and D. Nitz. *J. Chem. Phys.*, 124:244304, 2006.

[36] J. Christiansen, P. Heubes, R. Keitel, W. Klinger, W. Loeffler, W. Sandner, and W. Withhuhn. *Z. Phys. B*, 24:177, 1976.

[37] H. C. Verma. *Hyperfine Int.*, 15/16:207, 1983.

[38] M. Forker and L. Freise. *Hyperfine Int.*, 34:329, 1987.

[39] (***suitable reference to be found).

[40] P. Blaha, K. Schwarz, and P. Herzig. *Phys. Rev. Lett.*, 54(11):1192–1195, Mar 1985.

[41] P. Blaha, K. Schwarz, and P. H. Dederichs. *Phys. Rev. B*, 37(6):2792–2796, Feb 1988.

[42] Hisazumi Akai, Masako Akai, S. Blügel, B. Drittler, H. Ebert, Kiyoyuki Terakura, R. Zeller, and P. H. Dederichs. *Progress of Theoretical Physics Supplement*, 101:11, 1990.

[43] A. Svane, N. E. Christensen, C. O. Rodriguez, and M. Methfessel. *Physical Review B*, 55(18):12572, 1997.

[44] S. Lany, P. Blaha, J. Hamann, V. Ostheimer, H. Wolf, and T. Wichert. *Phys. Rev. B*, 62(4):R2259–R2262, Jul 2000.

[45] H. M. Petrilli, P. E. Blochl, P. Blaha, and K. Schwarz. *Physical Review B*, 57(23):14690–14697, 1998.

[46] S. J. Asadabadi, S. Cottenier, H. Akbarzadeh, R. Saki, and M. Rots. *Phys. Rev. B*, 66(19):195103, Nov 2002.

[47] S. Cottenier, V. Bellini, M. Çakmak, F. Manghi, and M. Rots. *Phys. Rev. B*, 70(15):155418, Oct 2004.

[48] M. Iglesias, K. Schwarz, P. Blaha, and D. Baldomir. *Phys. Chem. Minerals*, 28(67):67–75, 2001.

[49] M. R. Hansen, G. K. H. Madsen, H. J. Jakobsen, and J. Skibsed. *J. Phys. Chem. B*, 110(5975), 2006.

[50] F. Haarmann, K. Koch, D. Grüner, W. Schnelle, O. Pecher, R. Cardoso-Gil, H. Borrmann, H. Rosner, and Y. Grin. *Chem. Eur. J.*, 15:1673–1684, 2009.

[51] D. Kasinathan, A. Ormeci, K. Koch, U. Burkhardt, W. Schnelle, A. Leithe-Jasper, and H. Rosner. *New J. Phys.*, 11:025023, 2009.

[52] P. Jeglič, J.-W. G. Bos, A. Zorko, M. Brunelli, K. Koch, H. Rosner, S. Margadonna, and D. Arčon. *Phys. Rev. B*, 79:094515, 2009.

[53] V. Kellö and A. J. Sadlej. *Chem. Phys. Lett.*, 292:403, 1998.

[54] V. Kellö and A. J. Sadlej. *Mol. Phys.*, 96:275, 1998.

[55] V. Kellö, A. J. Sadlej, P. Pyykkö, D. Sundholm, and M. Tokman. *Chem. Phys. Lett.*, 302:414, 0999.

[56] V. Kellö and A. J. Sadlej. *Phys. Rev. A*, 60:3575, 1999.

[57] V. Kellö, P. Pyykkö, A. J. Sadlej, P. Schwerdtfeger, and J. Thyssen. *Chem. Phys. Lett.*, 318:222, 2000.

[58] M. Pernpointer, P. Schwerdtfeger, and B. A. Hess. *J. Chem. Phys.*, 108, 1998.

[59] V. Kellö and A. J. Sadlej. *Collect. Czech. Chem. Commun.*, 72:64–82, 2007.

[60] C. Thierfelder, P. Schwerdtfeger, and T. Saue. *Phys. Rev. A*, 76:034502, 2007.

[61] D. Torumba, K. Parlinski, M. Rots, and S. Cottenier. *Phys. Rev. B*, 74:144304, 2006.

[62] P. Schwerdtfeger, R. Bast, M. C. L. Gerry, C. R. Jacob, M. Jansen, V. Kellö, A. V. Mudring, A. J. Sadlej, T. Saue, T. Söhnel, and F. E. Wagner. *The Journal of Chemical Physics*, 122:124317, 2005.

[63] J. Cederberg, J. Nichol, E. Frodermann, H. Tollerud, G. Hilk, J. Buysman, W. Kleiber, M. Bongard, J. Ward, K. Huber, T. Khanna, J. Randolph, and D. Nitz. *J. Chem. Phys.*, 123:134321, 2005.

[64] C. Schlier. *Fortschr. Phys.*, 9:455, 1961.

[65] J. L. Dunham. *Phys. Rev.*, 41:721, 1932.

[66] P. Dufek, P. Blaha, and K. Schwarz. *Physical Review Letters*, 75:3545, 1995.

[67] Vladimir Kellö, Andrzej J. Sadlej, and Pekka Pyykkö. *Chemical Physics Letters*, 329:112, 2000.

[68] L. Errico, G. Darriba, M. Renteria, Z.N. Tang, H. Emmerich, and S. Cottenier. *Phys. Rev. B*, 77:195118, 2008.

[69] Giampaolo Barone, Remigius Mastalerz, Markus Reiher, and Roland Lindh. *The Journal of Physical Chemistry A*, 112(7):1666, 2009.

[70] S. Büttgenbach. *Hyperfine Int.*, 20:1–64, 1984.

[71] J. R. Crespo López-Urrutia, P. Beiersdorfer, K. Widmann, B. B. Birkett, A.-M. Mårtensson-Pendrill, and M. G. H. Gustavsson. *Phys. Rev. A*, 57(2):879–887, Feb 1998.

[72] J. Cederberg, D. Olson, J. Larson, G. Rakness, K. Jarausch, J. Schmidt, B. Borovsky, P. Larson, and B. Nelson. *Phys. Rev. A*, 57(4):2539–2543, Apr 1998.

[73] G. Paquette, A. Kotz, J. Cederberg, D. Nitz, A. Kolan, D. Olson, K. Gunderson, S. Lindaas, and S. Wick. The hyperfine spectrum of kf. *Journal of Molecular Structure*, 190:143 – 148, 1988.

[74] J. Cederberg, J. Randolph, B. McDonald, B. Paulson, and C. McEachern. *J. Mol. Spec.*, 250:114, 2008.

[75] J. Cederberg, S. Fortman, B. Porter, M. Etten, M. Feig, M. Bongard, and L. Langer. *J. Chem. Phys.*, 124:244305, 2006.

[76] H. Haken and H. C. Wolf. *Atom- und Quantenphysik.* Springer, 2003.

[77] J. M. B. Kellogg, I. I. Rabi, N. F. Ramsey Jr., and J. R. Zacharias. *Phys. Rev.*, 57:677, 1940.

[78] H. M. Foley. *Phys. Rev.*, 72:504, 1947.

[79] N. F. Ramsey. *Phys. Rev.*, 89:527, 1953.

[80] P. Pyykkö. *J. Phys. F: Metal Physics*, 1:102, 1971.

[81] U. Ganiel and S. Shtrikman. *Phys. Rev.*, 167(2):258–270, Mar 1968.

[82] R. Kamal and R.G. Mendirat. *Journal Of Physics And Chemistry Of Solids*, 31(4):872–&, 1970.

[83] P.A. Bonczyk. *Physics Letters A*, A 31(9):509–&, 1970.

[84] F. C. De Lucia, P. Helminger, and W. Gordy. *Phys. Rev. A*, 3(6):1849–1857, Jun 1971.

[85] K. V. Chance, T. D. Varberg, K. Park, and L. R. Zink. *J. Mol. Spec.*, 162:120, 1993.

[86] T. D. Varberg, J. C. Roberts, K. A. Tuominen, and K. M. Evenson. *J. Mol. Spec.*, 191:384, 1998.

[87] Wei Lin, Sara A. Beaton, Corey J. Evans, and Michael C.L. Gerry. *Journal of Molecular Spectroscopy*, 199(2):275 – 283, 2000.

[88] S. G. Batten and A. C. Legon. *Chemi. Phys. Lett.*, 422:192, 2006.

[89] W. Lin, C. J. Evans, and M. C. L. Gerry. *Physical Chemistry Chemical Physics*, 2:43, 2000.

[90] J. Cederberg, J. Ward, G. McAlistera, G. Hilk, E. Beall, and D. Olson. *Journal of Chemical Physics*, 111:8396, 1999.

[91] F. Matsushima, S. Kakihata, and K. Takagi. *J. Chem. Phys.*, 94:2408, 1991.

[92] D. Rybicki, J. Haase, M. Greven, G. Yu, Y. Li, Y. Cho, and X. Zhao. *Journal of superconductivity and novel magnetism*, 22:179, 2009.

[93] R. J. Rafac, B. C. Young, J. A. Beall, W. M. Itano, D. J. Wineland, and J. C. Bergquist. Sub-dekahertz ultraviolet spectroscopy of 199$hg+$. *Phys. Rev. Lett.*, 85(12):2462–2465, Sep 2000.

[94] S. Cottenier and M. Rots. *Hyperfine Interactions and their Application in Nuclear Condensed Matter Physics: a microscopic Introduction.* unpublished lecture notes Katholieke Universiteit Leuven, 2005.

[95] A. D. McNaught and A. Wilkinson. *IUPAC. Compendium of Chemical Terminology.* Blackwell Scientific Publications, Oxford, 1997.

[96] The term "quadrupole shift" can appear in the literature with another meaning than the one defined in this paper. In NQR, it sometimes refers to the anisotropy of the quadrupole interaction with the applied field [92], while in high-precision optical spectroscopy it refers to the interaction between an atom's nucleus and the background electric-field gradient provided by an ion trap [93] .

[97] To exploit the quadrupole shift (see Sec. VI) for muonic atoms, however, is not possible since no such experiments have been published for a couple of decades and the apparatus has been demounted [27].

[98] For all spherical tensors of rank two with a three, four or six fold rotation axis it can be shown, that only the $m = 0$ component is nonzero (which is equivalent to $\eta = 0$) [94]. This means, if $\eta = 0$ then also $\eta_{QS} = 0$ and vice versa.

[99] Note, that in Ref. [24], the root-mean-square (RMS) of the nuclear radius is given, while here we use the monopole radius.

[100] Most of the literature in this context uses the word 'isotopomers' to refer to (e.g.) the pair $^7Li^{127}I$ and $^6Li^{127}I$. According to the 1994 IUPAC recommendations [95], 'isotopologues' is the better term for this.